



Proximity plasma excitations in disk and ring geometries

V. M. Muravev,¹ A. M. Zarezin ^{1,2} P. A. Gusikhin,¹ A. V. Shupletsov ³ and I. V. Kukushkin¹

¹*Institute of Solid State Physics, RAS, Chernogolovka, 142432 Russia*

²*Moscow Institute of Physics and Technology, Dolgoprudny, 141700 Russia*

³*P. N. Lebedev Physics Institute, 119991 Moscow, Russia*



(Received 30 August 2019; published 5 November 2019)

We have investigated plasma excitations in the hybrid system with a disk-shaped metallic gate introduced on top of an infinite two-dimensional electron system. The proximity plasma excitations have been identified and explored in this partially-gated system, and the results are compared with the behavior of ordinary gated plasmons excited in a system with the disk geometry. Significantly, with the change of the gate geometry from a disk to a narrow ring, we observed the transformation of proximity plasmons with linear dispersion into those having square-root dependence on the wave vector. Our experimental findings show good agreement with the theory.

DOI: [10.1103/PhysRevB.100.205405](https://doi.org/10.1103/PhysRevB.100.205405)

I. INTRODUCTION

Recently, a new electromagnetic plasma mode has been discovered in the hybrid system constructed by putting a highly conductive gate strip in proximity to the two-dimensional electron system (2DES) [1,2]. It was found that such a proximity plasmon mode propagates along the gate strip without any potential nodes in the transverse direction. The proximity plasmon mode differs significantly from the conventional gated and ungated 2D plasma modes that have been known in the literature for more than half a century [3–8]. The dispersion of the proximity plasmon mode has been described in Ref. [2] as:

$$\omega_{\text{pr}}(q) = \sqrt{\frac{2n_s e^2 h}{m^* \epsilon \epsilon_0} \frac{q}{W}} \quad (qW \ll 1), \quad (1)$$

where n_s is the 2D electron density, m^* is the effective electron mass, h is the distance between the gate and the 2DES, W is the width of the gate strip, q is the plasmon wave vector along the gate, and ϵ is the effective dielectric permittivity of the semiconductor crystal ($\epsilon = 12.8$ for GaAs). The electric field and the potential of the proximity plasma wave are highly delocalized in the direction perpendicular to the gate strip with the delocalization distance determined by the plasmon wavelength along the strip.

By contrast, an ordinary gated plasmon is largely confined to the region directly underneath the gate, and for an infinite 2DES, its spectrum takes the linear form [4]

$$\omega_g(q) = \sqrt{\frac{n_s e^2 h}{m^* \epsilon \epsilon_0}} q \quad (qh \ll 1). \quad (2)$$

Gated plasmons are regarded very promising because of their ability to concentrate the electric field of the incident electromagnetic wave in the nanogap between the 2DES and the gate. Therefore, this type of plasma excitation has been studied extensively in numerous experimental works [9–13].

In this paper, we investigate how the proximity plasmon modifies its behavior as its gate geometry is changed from

a strip ($qW \ll 1$) to a disk ($qW \sim 1$). We conducted our experiments on the infinite 2DES with a single metallic disk fabricated on top of the chip. Thus far, plasma excitations in this kind of a system have remained unexplored mainly due to the fact that its geometry is reciprocal to the common one of a finite 2DES and an infinite screening gate [9,14–16]. In the course of our study, we identified and investigated the proximity plasma modes excited in the disk-shaped gate geometry. We demonstrate that plasmons localized in the vicinity of the gate exist even with zero gate voltage and with preserved 2DES homogeneity. The proximity plasmon in the disk-shaped geometry exhibits a linear dispersion. Furthermore, given the linear dispersion of the plasmon excitation, we show that changing the gate shape from a disk to a narrow ring results in recovery of the square-root proximity plasmon dispersion observed initially in the case of a strip gate configuration.

II. EXPERIMENTAL TECHNIQUE

The samples under study were fabricated from GaAs/AlGaAs heterostructure hosting a two-dimensional electron system in a 30 nm wide quantum well located at the depth $h = 440$ nm below the crystal surface. For the set of different samples from the same wafer, the electron density was equal to $n_s = (2.4\text{--}2.8) \times 10^{11} \text{ cm}^{-2}$ with the low-temperature mobility reaching approximately $5 \times 10^6 \text{ cm}^2/\text{V s}$. Each sample was lithographically patterned into the Corbino geometry as depicted in Fig. 1(b). The outer Au/Ge contact was made 1 mm \times 1 mm square with a round center gap of diameter $D = 0.5$ mm. The 2DES resided within the opening, with the gate of diameter d fabricated in the center. The gate size was varied between the samples, with $d = 50, 100,$ and $200 \mu\text{m}$. For the measurements, we used the microwave radiation in the range of 1–40 GHz. The signal was guided to the center gate through a coaxial cable with matched impedance while the contact itself was grounded. To prevent physical damage to the gate, a bonding wire was connected to it with conductive epoxy glue. In order to

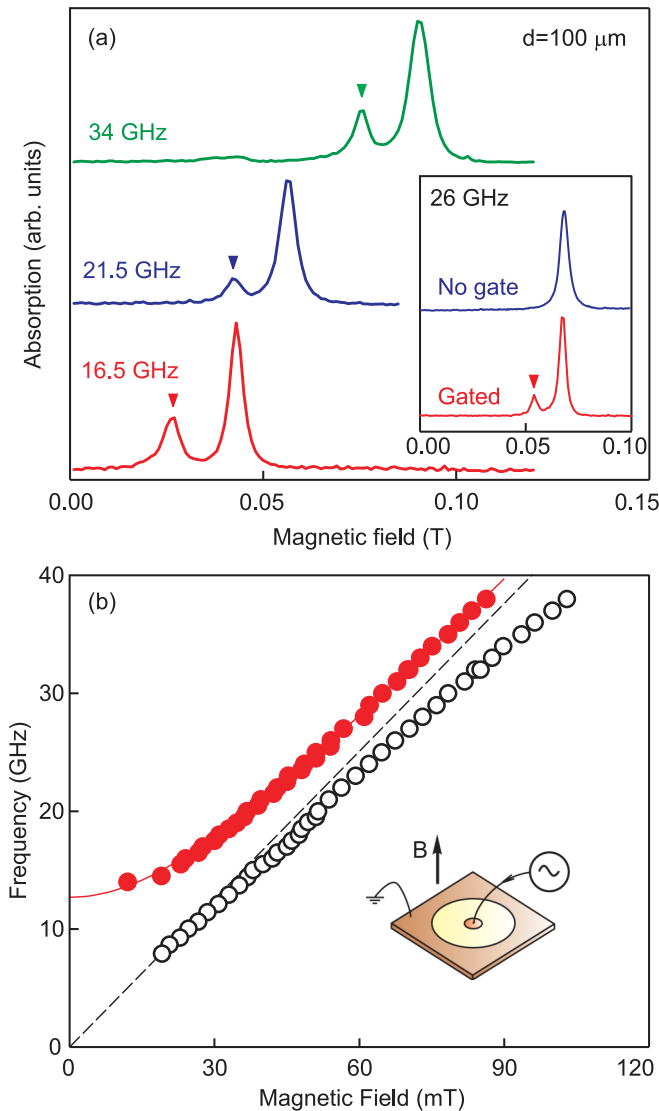


FIG. 1. (a) Microwave absorption as a function of the applied magnetic field, plotted for the incident microwave radiation of 16.5, 21.5, and 34 GHz and for $d = 0.1$ mm. The curves are normalized and shifted for clarity with the arrows marking the resonance under consideration. (b) Comparison of the magnetodispersion of the proximity plasmon mode (red circles) to that of a single-particle (CR) resonance (empty circles). The solid red line represents the theoretical curve given by Eq. (3) while the dashed line indicates the CR position. The inset displays a schematic view of the device with the excitation circuit.

detect the microwave absorption, we employed a noninvasive optical technique [17,18] (see Supplemental Material I [19] and references [9,14,17,18,20–22] therein), for which the sample was placed inside the superconducting coil with the base temperature of 1.5 K.

III. EXPERIMENTAL RESULTS

Figure 1(a) illustrates typical microwave absorption spectra measured as a function of the externally applied magnetic field B . The measurements were carried out at 16.5, 21.5,

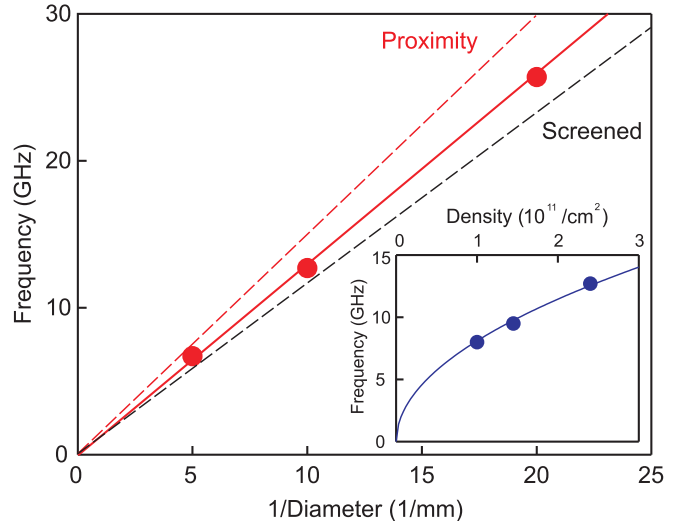


FIG. 2. Plots of the proximity plasmon dispersion obtained from testing the samples with different gate diameters, $d = 50, 100$ and $200 \mu\text{m}$ and constant $n_s = 2.4 \times 10^{11} \text{cm}^{-2}$. The solid red line denotes a linear fit to the experimental data. The dashed lines show the calculated dispersion of the proximity plasmon based on Eq. (4) and the gated 2D plasmon according to Eq. (5). The inset displays the plasmon frequency dependence on the electron density measured for the samples with gate diameter $d = 100 \mu\text{m}$. The solid blue curve designates a square-root fit to the theoretical data.

and 34 GHz for the sample with center gate diameter, $d = 0.1$ mm. Each curve exhibits two major resonances (detailed analysis of additional minor resonances is given in Supplemental Material II [19]). The more prominent peak closely follows the cyclotron resonance (CR) defined by $\omega_c = eB/m^*$, as indicated with the empty circles in Fig. 1(b). The physical origin of this single-particle resonance is still far from being unequivocal [23,24]. The secondary resonance, on the other hand, as marked by the arrows in Fig. 1(a), is excited only in the presence of a disk-shaped gate [see inset to Fig. 1(a)]. Therefore, we attribute this resonance to the excitation of the proximity plasmon [1,2]. Its magnetodispersion is shown in Fig. 1(b) by red circles. The experimentally obtained magnetodispersion possesses two distinctive features. Firstly, the data are well described by:

$$\omega^2 = \sqrt{\omega_c^2 + \omega_{\text{pr}}^2}, \quad (3)$$

where ω_{pr} is the plasmon frequency at zero magnetic field. Secondly, the plasmon excitation under investigation has no edge magnetoplasmon mode in the presence of a magnetic field [9,25–27]. Both of these peculiarities are characteristic of the proximity plasmon, setting it apart from the well-established screened plasmon, observed in the 2DES disk screened by an infinite gate [9,28].

For a complete picture, experiments of Fig. 1 have been carried out on three samples with different diameter of the center gate, $d = 50, 100$, and $200 \mu\text{m}$. Figure 2 displays the resultant dependency of $\omega_{\text{pr}}(B = 0)$ on the parameter $1/d$. Obtained spectrum of the proximity plasmon in the disk geometry is linear. The theoretical analysis of the proximity plasmons excited in an infinite 2DES screened by a

disk-shaped metallic gate [29] yields the following expression

$$\omega_{\text{pr}} = \Omega \sqrt{\frac{n_s e^2 \hbar}{m^* \epsilon \epsilon_0} \frac{2}{d}}, \quad (4)$$

where $\epsilon = \epsilon_{\text{GaAs}} = 12.8$ and the dimensionless frequency Ω is determined from the equation: $\partial_{\Omega} J_{|m|}(\Omega) + |m| J_{|m|}(\Omega) / \Omega = 0$ [29], with $J_{|m|}(x)$ denoting the Bessel function of the first kind. In the case of the fundamental proximity plasmon mode, with $m = 1$, this equation gives $\Omega = 2.4$ and the corresponding dispersion depicted in Fig. 2 by the dashed line, indicating a remarkable agreement between the experimental data and the theory. Here, a minor discrepancy can be ascribed to an inaccurate description of the dielectric environment surrounding the 2DES. The inset to Fig. 2 illustrates the dependence of the proximity plasmon frequency on the electron density, n_s , measured for the sample with the gate diameter $d = 100 \mu\text{m}$. Clearly, the data points are perfectly fitted with the curve of a square-root dependence.

It should be noted that the spectrum in (4) is similar to the plasmon dispersion of the “inverse” system geometry, i.e., with the 2DES in the form of a disk placed under an infinite gate. For such a system, the gated plasmon dispersion has been described in Ref. [14] as:

$$\omega_g = \alpha \sqrt{\frac{n_s e^2 \hbar}{m^* \epsilon \epsilon_0} \frac{2}{d}}, \quad (5)$$

where $\alpha = 1.84$ is the first zero of the $J_1'(x)$ Bessel function. In both (4) and (5) the spectra exhibit identical linear dependence on the wave vector $q = 2/d$, differing merely by a numerical factor, as indicated by the dashed lines in Fig. 2.

The close resemblance of the modes observed in the aforementioned disk-shaped geometries is due to the fact that in either configuration, the plasmon energy density is localized primarily under the gated area reaching its maximum at the disk center. In fact, the only difference between the modes lies in their boundary conditions around the edge of the disk where the field is relatively small. This explains the apparent similarity between the spectra of the gated and the proximity plasmons in Fig. 2. It is this circumstance that has frequently led to the confusion of these two completely different types of plasma excitations [23].

To further highlight the difference between the gated and the proximity plasmons, we experimented with a series of samples having an aperture in the 2DES under the gate, as shown in the inset in Fig. 3(b). The aperture is created by chemical etching of the semiconductor chip. The samples had a fixed overlap between the gate and the 2DES, constant rim width $W = 5 \mu\text{m}$, and different gate diameters $d = 50, 100,$ and $200 \mu\text{m}$. The resultant configuration is analogous to the ring geometry in terms of the 2DES under the gate. In fact, the given arrangement is topologically equivalent to a looped strip gate considered in Refs. [1,2]. Based on Eq. (1), one would expect that in such a geometry, the proximity plasmon should have a square-root spectrum, whereas the gated plasmon should have a linear dispersion defined by Eq. (2).

Figure 3(a) illustrates the magnetodispersion of the proximity plasmon excitation for the ring-shaped samples with the gate diameter $d = 50$ and $100 \mu\text{m}$ plotted by the blue and red dots, correspondingly. Remarkably, each magnetodispersion

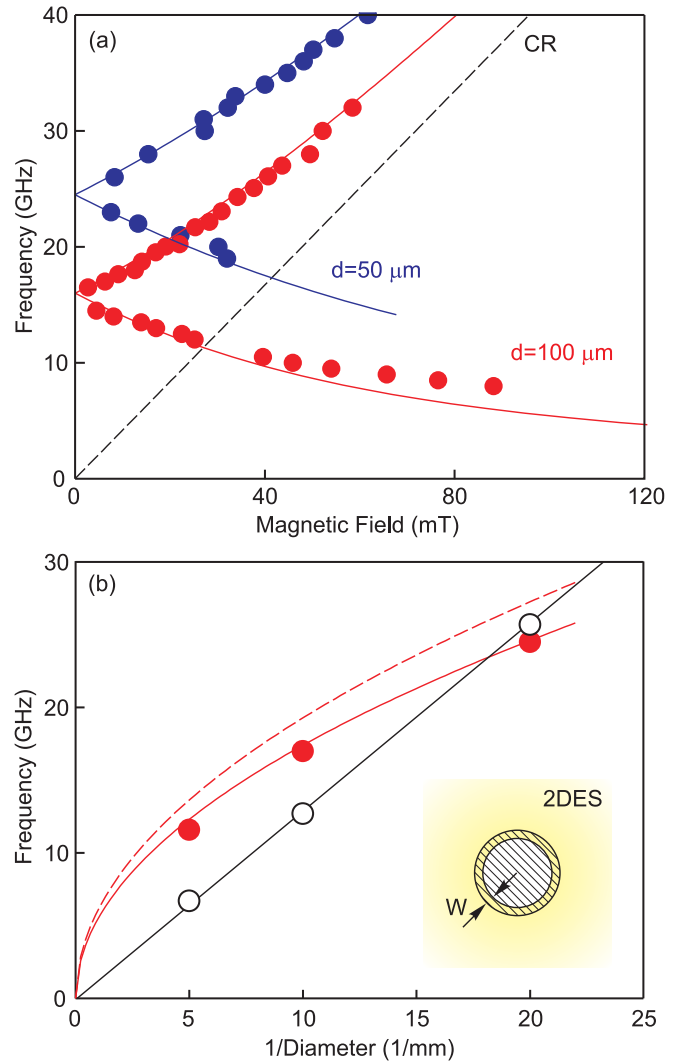


FIG. 3. (a) Magnetodispersion of the proximity plasmon modes in a ring geometry measured for the gate diameter $d = 50$ and $100 \mu\text{m}$ (blue and red circles, respectively) and a fixed ring width $W = 5 \mu\text{m}$. The solid curves represent the theoretical data from Eq. (6). (b) Comparison of the proximity plasmon spectra measured for the ring geometry (red circles) and the disk geometry (empty circles; data from Fig. 2). The inset depicts a schematic view of the sample under study with W denoting the ring width, the yellow color designating the 2DES with an aperture, and the hatched area corresponding to the metallic gate.

consists of two branches. The upper branch in the high-frequency limit tends to the cyclotron resonance asymptote. The lower branch, on the other hand, exhibits frequency falloff with increasing magnetic field—the characteristic behavior of the edge magnetoplasmon (EMP). EMP is a plasma wave propagating along the edge of the 2DES in the direction determined by the external B field [9,25–27] with its velocity being proportional to the Hall conductivity $\sigma_{xy} \propto n_s/B$. In this regard, it has been shown that proximity plasmons excited in an infinite 2DES do not have the EMP mode [1,2] for the simple reason that in this case, the 2DES has no edge.

In our experiments, however, the etching of the disk interior creates the edge necessary to support the EMP mode

of the proximity plasmon. In practice, we found that the magnetodispersion of both modes can be well described by a straightforward dipole approximation [25] as illustrated in Fig. 3(a):

$$\omega = \pm \frac{\omega_c}{2} + \sqrt{\omega_{\text{pr}}^2 + \left(\frac{\omega_c}{2}\right)^2}. \quad (6)$$

In Fig. 3(b), we summarize the dependency of the plasma excitation frequency on the inverse of the disk diameter, $1/d$, as indicated with the red dots. Importantly, the resultant square-root dispersion is a characteristic feature of the proximity plasmon. For the purpose of comparing the experimental data with the theory, the dashed line in the figure represents the dispersion calculated from Eq. (1) for $q = 2/d$. Here, it should be noted that the calculations take into account the fact that 2DES is located only on one side of the gated area. Therefore, the coefficient of 2 in the numerator of Eq. (1) should be omitted. Similar to the results displayed in Fig. 2, the current plots evidence minor discrepancy between the experimental data and the theoretical prediction. By and large, in Fig. 3(b) we demonstrate the conversion of the proximity plasmon spectrum from a square-root form for a strip gate geometry, as marked with the solid circles, to a linear form for a disk gate configuration, as denoted with the empty circles.

IV. CONCLUSIONS

In conclusion, resonant microwave absorption has been investigated in the two-dimensional electron system with a highly conductive gate disk placed in proximity to the 2DES. We have found new plasma excitation localized near the gate. Even though its frequency is of the same order as that of the conventional gated plasmons excited in the screened disk-shaped 2DES, we demonstrated that the physical origin of the two modes is completely different. We have provided experimental evidence by testing the same set of samples but with an aperture in the 2DES under the gate. We have shown that the change in the sample geometry from a disk-shaped gate to that of a narrow ring results in recovery of the square-root proximity plasmon dispersion.

ACKNOWLEDGMENTS

We thank V. A. Volkov and A. A. Zabolotnykh for the stimulating discussions. We are also grateful to V. N. Zverev for his assistance with sample preparation. This work was supported by the Russian Science Foundation (Grant No. 19-72-30003).

-
- [1] V. M. Muravev, P. A. Gusikhin, A. M. Zarezin, I. V. Andreev, S. I. Gubarev, and I. V. Kukushkin, *Phys. Rev. B* **99**, 241406(R) (2019).
- [2] A. A. Zabolotnykh and V. A. Volkov, *Phys. Rev. B* **99**, 165304 (2019).
- [3] F. Stern, *Phys. Rev. Lett.* **18**, 546 (1967).
- [4] A. V. Chaplik, *Zh. Eksp. Teor. Fiz.* **62**, 746 (1972) [*Sov. Phys. JETP* **35**, 395 (1972)].
- [5] C. C. Grimes and G. Adams, *Phys. Rev. Lett.* **36**, 145 (1976).
- [6] S. J. Allen, Jr., D. C. Tsui, and R. A. Logan, *Phys. Rev. Lett.* **38**, 980 (1977).
- [7] T. N. Theis, J. P. Kotthaus, and P. J. Stiles, *Solid State Commun.* **24**, 273 (1977).
- [8] U. Mackens, D. Heitmann, L. Prager, J. P. Kotthaus, and W. Beinvogl, *Phys. Rev. Lett.* **53**, 1485 (1984).
- [9] D. C. Glatli, E. Y. Andrei, G. Deville, J. Poitrenaud, and F. I. B. Williams, *Phys. Rev. Lett.* **54**, 1710 (1985).
- [10] P. J. Burke, I. B. Spielman, J. P. Eisenstein, L. N. Pfeiffer, and K. W. West, *Appl. Phys. Lett.* **76**, 745 (2000).
- [11] V. M. Muravev, C. Jiang, I. V. Kukushkin, J. H. Smet, V. Umansky, and K. von Klitzing, *Phys. Rev. B* **75**, 193307 (2007).
- [12] W. F. Andress, H. Yoon, K. Y. M. Yeung, L. Qin, K. West, L. Pfeiffer, and D. Ham, *Nano Lett.* **12**, 2272 (2012).
- [13] D. A. Iranzo, S. Nanot, E. J. C. Dias, I. Epstein, C. Peng, D. K. Efetov, M. B. Lundberg, R. Parret, J. Osmond, J.-Y. Hong, J. Kong, D. R. Englund, N. M. R. Peres, and F. H. L. Koppens, *Science* **360**, 291 (2018).
- [14] Alexander L. Fetter, *Phys. Rev. B* **33**, 5221 (1986).
- [15] E. H. Hwang and S. Das Sarma, *Phys. Rev. B* **75**, 205418 (2007).
- [16] V. Ryzhii, A. Satou, and T. Otsuji, *J. Appl. Phys.* **101**, 024509 (2007).
- [17] B. M. Ashkinadze, E. Linder, and V. Umansky, *Phys. Rev. B* **62**, 10310 (2000).
- [18] V. M. Muravev, I. V. Andreev, S. I. Gubarev, V. N. Belyanin, and I. V. Kukushkin, *Phys. Rev. B* **93**, 041110(R) (2016).
- [19] See Supplemental Material at <http://link.aps.org/supplemental/10.1103/PhysRevB.100.205405> for additional experimental data on optical technique used for detection of the plasma resonances and analysis of additional minor resonances.
- [20] A. A. Zagitova, V. M. Muravev, P. A. Gusikhin, A. A. Fortunatov, and I. V. Kukushkin, *JETP Lett.* **108**, 446 (2018).
- [21] V. M. Muravev, I. V. Andreev, S. I. Gubarev, P. A. Gusikhin, and I. V. Kukushkin, *JETP Lett.* **109**, 663 (2019).
- [22] S. A. Mikhailov and N. A. Savostianova, *Phys. Rev. B* **74**, 045325 (2006).
- [23] I. V. Andreev, V. M. Muravev, V. N. Belyanin, and I. V. Kukushkin, *Phys. Rev. B* **96**, 161405(R) (2017).
- [24] S. I. Dorozhkin, A. A. Kapustin, I. A. Dmitriev, V. Umansky, K. von Klitzing, and J. H. Smet, *Phys. Rev. B* **96**, 155306 (2017).
- [25] S. J. Allen, Jr., H. L. Störmer, J. C. M. Hwang, *Phys. Rev. B* **28**, 4875 (1983).
- [26] D. B. Mast, A. J. Dahm, and A. L. Fetter, *Phys. Rev. Lett.* **54**, 1706 (1985).
- [27] V. A. Volkov and S. A. Mikhailov, *Sov. Phys. JETP* **67**, 1639 (1988).
- [28] S. I. Gubarev, V. M. Muravev, I. V. Andreev, V. N. Belyanin, and I. V. Kukushkin, *JETP Lett.* **102**, 461 (2015).
- [29] A. A. Zabolotnykh and V. A. Volkov, *Semiconductors* **53**, 4 (2019).